ELSEVIER

Contents lists available at ScienceDirect

Atmospheric Environment

journal homepage: www.elsevier.com/locate/atmosenv





Measurements of brown carbon and its optical properties from boreal forest fires in Alaska summer

Kunal Bali^a, Sujai Banerji^b, James R. Campbell^a, Aachal Vallabhbhai Bhakta^c, L.-W. Antony Chen^{d,e}, Christopher D. Holmes^c, Jingqiu Mao^{a,*}

- a Department of Chemistry and Biochemistry and Geophysical Institute, University of Alaska Fairbanks, Fairbanks, AK, USA
- ^b Institute for Atmospheric and Earth System Research/Physics, University of Helsinki, Helsinki, Finland
- ^c Department of Earth, Ocean and Atmospheric Science, Florida State University, Tallahassee, FL, USA
- ^d Department of Environmental and Occupational Health, University of Nevada, Las Vegas, NV, USA
- e Division of Atmospheric Sciences, Desert Research Institute, Reno, NV, USA

ARTICLE INFO

Keywords: Brown carbon Organic carbon Light absorption Mass absorption coefficient Wildfire Arctic

ABSTRACT

Brown carbon (BrC) plays an important role in global radiative budget but there have been few studies on BrC in Arctic despite rapid warming and increasing wildfires in this region. Here we investigate the optical properties of BrC from boreal fires in Alaska summer, with two sets of measurements from PILS-LWCC-TOC (Particle-Into-Liquid-Sampler – Liquid-Waveguide Capillary flow-through optical Cell - Total-Organic-Carbon analyzer) and filter measurements. We show that during intense wildfires, the mass absorption coefficient at 365 nm (MAC₃₆₅) from water soluble organic carbon (WSOC) remained stable at $\sim 1~{\rm m}^2~{\rm g}^{-1}$. With all plumes sampled and derived transport time, we show a decrease of MAC₃₆₅ with plume age, with a shorter photobleaching lifetime ($\sim 11~{\rm h}$) at 365 nm compared to 405 nm ($\sim 20~{\rm h}$). The total absorption by organic aerosols measured from filters at 365 nm is higher than the absorption by WSOC by a factor 2–3, suggesting a dominant role of insoluble organic carbon. Overall BrC dominates absorption in the near-ultraviolet and visible radiation during wildfire season in Alaska summer.

1. Introduction

Organic aerosols (OA) with strong absorption at near ultraviolet (UV) and short visible wavelengths (300–400 nm) are referred to as brown carbon (BrC) (Andreae and Gelencser, 2006; Feng et al., 2013, Yan et al., 2018; Laskin et al., 2015; Zeng et al., 2020, 2021). BrC is different from black carbon (BC), which tends to absorb at all visible wavelengths. BrC absorption can pose a significant warming effect (\pm 0.04 to \pm 0.5 W m \pm 2, global average) at the top of atmosphere (TOA), contributing to 7–48% of TOA-Direct Radiative Effect (TOA-DRE) (Zeng et al., 2022; Zhang et al., 2017). In particular, BrC can exert the largest DRE over the Arctic region (0.04 W m \pm 2), a factor of 2 higher than the global average (June et al., 2020).

Biomass burning, particularly those with lower combustion efficiencies, is one of the major sources of BrC globally (Healy et al., 2015; Laskin et al., 2015; Soleimanian et al., 2020; Yuan et al., 2020; Yue et al., 2022; Zeng et al., 2022). Boreal forest fires are expected to be rich in BrC

as smoldering duff comprises much of the fuel consumption (Akagi et al., 2011; Genet et al., 2018; Schmale et al., 2018; Turetsky et al., 2010, 2014). Other sources of BrC include biofuel and fossil fuel combustion which are more prominent in populated urban and suburban areas (Saleh et al., 2013, 2014; Yuan et al., 2020; Yue et al., 2019, 2022; Zhang et al., 2013).

Extensive measurements have been made in the past three decades to quantify the light absorption of aerosols associated with BrC. These measurements have been made broadly in three categories: measurements of optical properties of bulk aerosol material and extracts, measurements of transmission on aerosol filters, and direct measurements on aerosol optical properties (Laskin et al., 2015). The first category includes measurements on extracts from filters (Chen and Bond, 2010) or particle-into-liquid sampler (PILS) (Hecobian et al., 2010). The second category includes the particulate soot absorption photometer (PSAP) (Bond et al., 1999), the aethalometer (Hansen et al., 1984), and the multiangle absorption photometer (MAAP) (Petzold and Schönlinner,

E-mail address: jmao2@alaska.edu (J. Mao).

^{*} Corresponding author.

2004). The third category includes cavity-based methods such as cavity ring-down (CRD), cavity enhanced spectroscopy (CES) and photo-acoustic spectroscopy (PAS) (Lack et al., 2006; Washenfelder et al., 2013).

The measurements of BrC over the Arctic region are sparse despite the increasing trend of wildfire activities in this region (McCarty et al., 2021; Alaska Division of Forestry, 2019). Most measurements in Arctic are based on filter samples (Yue et al., 2019; 2022). McNaughton et al. (2011) used filter-based Particle Soot/Absorption Photometer (PSAP) measurements and a thermal denuder during ARCTAS (Arctic Research of the Composition of the Troposphere from Aircraft and Satellites) field campaign to indirectly derive of BrC mass absorption coefficient of 0.83 $m^2 g^{-1}$ and 0.27 $m^2 g^{-1}$ at 470 nm and 530 nm, respectively. However, their samples included smoke from cropland and boreal forest fires, so these results are not specific to boreal forest fires. Corr et al. (2012) found enhanced absorption at UV wavelength compared to visible wavelength in long-range transported biomass burning plumes (ARC-TAS-A) and those from boreal forests in Canada (ARCTAS-B). Differences in wavelength dependence of absorption between ARCTAS-A/B were attributed to differences in plume age and OA/BC ratio from different biomass burning sources. Laboratory burning of Alaska peatlands and duff are also found to emit significant amounts of BrC relative to BC (Chakrabarty et al., 2016; Sumlin et al., 2017; Watson et al., 2019). However, there are few in-situ high time-resolution measurements available on BrC from boreal forest fires.

One main uncertainty in quantifying the role of BrC on radiative forcing is its lifetime. Studies reported that BrC absorption decays with time in the presence of sunlight, known as the photobleaching effect (Forrister et al., 2015; Lee et al., 2014). Laboratory and field studies suggest that the timescale of photobleaching varies from hours (Lee et al., 2014; Sullivan et al., 2022; Washenfelder et al., 2022; Wong et al., 2017; Zeng et al., 2022; Zhao et al., 2015) to days (Lin et al., 2016; Sumlin et al., 2017; Zhong and Jang, 2014) and months (Fleming et al., 2020; Kristiansen et al., 2016; Zeng et al., 2022). Recent field studies on wildfires in mid-latitude also suggest that fresh smoke has minimum photobleaching of BrC in the first 5-10 h (Sullivan et al., 2022; Washenfelder et al., 2022; Zeng et al., 2022). If photobleaching or heterogeneous oxidation via hydroxyl radical is the major pathway for BrC photobleaching (Laskin et al., 2015) then these processes are potentially to be slower at high latitudes because of the reduced availability of UV radiation, leading to a longer lifetime of BrC in the high latitudes.

Boreal forest fires in Alaska occur mostly between the Alaska and Brooks ranges, where hot and dry summer conditions coincide with substantial biomass (Potter et al., 2021). Located in interior Alaska, Fairbanks is exposed to heavy smoke from boreal forest fires nearly every summer, with an increasing trend over the past few decades (Veraverbeke et al., 2017). Biomass burning is the dominant contributor to organic aerosols in Fairbanks summer (Deshmukh et al., 2019). However, the complex terrain in Alaska makes it challenging to use the long-term observational sites to evaluate the BrC from wildfires in Alaska. For example, several Interagency Monitoring of PROtected Visual Environments (IMPROVE) sites in Alaska are located south of Alaska range, where air masses are much less influenced by boreal forest fires (June et al., 2020). Thus, ground-based measurements in Fairbanks provide unique opportunities to examine BrC from boreal forest fires.

Here we show the in-situ measurements of water-soluble brown carbon from a non-filter PILS-LWCC-TOC instrument deployed in Fairbanks in the summer of 2019, combined with multiple-wavelength analysis of filters collected from the Alaska Department of Environmental Conservation's national core (ADEC NCORE) site in downtown Fairbanks, to better understand the BrC and its optical properties from boreal forest fires in Alaska summer.

2. Measurements

2.1. PILS-LWCC-TOC

During the summer of 2019, we deployed a particle into a liquid sampler (PILS, Brechtel Model 4001), coupled with a liquid waveguide capillary flow-through optical cell (LWCC) and Total Organic Carbon analyzer (TOC, Sievers Model 900), to measure water soluble organic carbon and its absorption over the range from 200 nm to 800 nm in real time. This PILS-LWCC-TOC system was deployed at a trailer next to the EPA NCORE site (longitude -147.72, latitude 64.84) in downtown Fairbanks, from 26 May to July 30, 2019. Our instrument setup largely follows previous studies (Hecobian et al., 2010; Sullivan et al., 2004; Weber et al., 2001) and it is briefly described here.

Ambient air is sampled by PILS (particle-into-liquid sampler) through a cyclone inlet at flow rate of 15 L/min to remove particles larger than 2.5 µm aerodynamic diameter. The air flow is then mixed with a hot steam generated with Milli-Q water. The turbulent mixing of hot steam with ambient air leads to a rapid cooling and supersaturation of water vapor, allowing ambient particles grow into large droplets. These droplets are subsequently collected on an inertial impactor surface and pumped into LWCC (liquid waveguide capillary cell) at a liquid flow rate of 0.5 L/min for measurement of absorption over a wavelength range of 200-800 nm. The UV-VIS light absorption spectra of the liquid samples are measured by a LWCC with a long path length (100 cm) (World Precision Instruments), coupled with a UV-VIS light source (Ocean Optics), and a multi-wavelength light detector (USB4000 Miniature Fiber Optic Spectrometer, Ocean Optics). Complete light absorption spectra between wavelengths of 200 and 800 nm of the liquid sample are recorded with a UV/VIS spectrometer. The flow coming out of LWCC is subsequently measured by a TOC (Total Organic Carbon) analyzer (Sievers M9) for water soluble organic carbon concentrations. The PILS-LWCC-TOC method is able to measure water soluble BrC, every 20 s, directly in aerosol solutions. This method can isolate BrC from BC and mineral dust that are not soluble in water. The schematic diagram and temporal resolution of PILS-LWCC-TOC are in the supplementary material (Fig. S1, Table S1).

The light absorption at a given wavelength (A_{λ}) from liquid sample is measured by the spectrometer following Beer's law:

$$A_{\lambda} = -\log_{10}(I/I_0) \tag{1}$$

where the transmitted (I) and incident (I₀) light intensity at wavelength λ are obtained from the liquid sample and Milli-Q water respectively. We calculate the absorption coefficient at a given wavelength (abs $_{\lambda}$) largely following Hecobian et al. (2010):

$$abs_{WSOC,\lambda} = (A_{\lambda} - A_{600}) \frac{V_1}{V_n \times L} \bullet ln(10)$$
 (2)

where WSOC stands for the water-soluble organic carbon (WSOC), V_1 is the PILS liquid sample flow rate (0.5 mL/min) and Va is the air sampling flow of 15 L/min, L is the absorbing path length of approximately 1 m, and A_{600} is the light absorption at 600 nm. Here we choose the absorption at 600 nm (mean between 595 nm and 605 nm) rather than 700 nm to zero the blank light absorption measurements, as our spectrometer shows higher noise level at 700 nm than at 600 nm when the trailer was hot in summer. We can further compute the WSOC MAC (MACWSOC, λ) at a given time as:

$$MAC_{WSOC,\lambda} = \frac{abs_{WSOC,\lambda}}{[WSOC]}$$
 (3)

where [WSOC] is the concentration of WSOC measured by TOC analyzer at a time resolution of 4 min. Combined with light spectra, our instrument can measure $abs_{WSOC, \lambda}$ and $MAC_{WSOC, \lambda}$ at a 4-min time resolution. During the analysis of $MAC_{WSOC,365}$, we set the high TOC background values of 52 ppb applied for wildfire events, and low TOC background

values of 10 ppb applied for clean conditions. This approach helps to minimize the uncertainty associated with WSOC and MAC calculation, particularly during clean conditions. The relative uncertainties associated with measured WSOC and abs_WSOC,365 are estimated to be 9% and 11% for the wildfire period (PM2.5 > 10 μg m $^{-3}$) and 35% and 8% for clean days (PM2.5 < 5 μg m $^{-3}$), respectively. These uncertainties are comparable to the uncertainties reported by Zeng et al. (2021, 2022) and Sullivan et al. (2004), which documented uncertainty ranges of 12%–16% for abs_WSOC,365 and 5–10% for WSOC from the PILS-LWCC-TOC instrument.

One major advantage of deploying PILS-LWCC-TOC instrument next to EPA NCORE site is that we can take advantage of a large suite of hourly gas and aerosol measurements, including carbon monoxide (CO), reactive nitrogen compounds (NO $_y$) (NO $_x$ data is not available), sulfur dioxide (SO $_2$), PM2 $_5$ mass concentrations, and meteorological parameters. These NCORE data are readily available from EPA air quality system (https://www.epa.gov/aqs).

2.2. National core monitoring sites (NCORE) filter analysis

We also take advantage of brown carbon filter analysis that is conducted for NCORE site. As part of NCORE measurements, carbonaceous aerosol in ambient particulate matter less than 2.5 μm (PM $_{2.5}$) are sampled onto quartz-fiber filters through URG 3000 N carbon sampler, for one 24-hr period every three days. The filters for the period of 2016–2019 were analyzed at Desert Research Institute (DRI) using a multiwavelength thermal/optical analyzer (Chow et al., 2015; Chen et al., 2015). Total carbon (TC), elemental carbon (EC), organic carbon (OC), and light absorption coefficient at seven wavelengths (i.e., 405, 445, 532, 635, 780, 808, and 980 nm) were reported. With prescribed absorption profiles for black carbon (BC) and brown carbon (BrC), we apportion TC into BC, BrC and white carbon (WtC) following Chen et al. (2021):

$$[TC] = [BC] + [BrC] + [WtC]$$
(4)

afterward absorption coefficient was estimated via:

$$abs_{\lambda} = MAC_{BC,\lambda} \times [BC] + MAC_{BrC,\lambda} \times [BrC]$$
(5)

where MAC $_{BC,\ \lambda}$ and MAC $_{BrC},\ \lambda$ are the wavelength-specific mass absorption efficiency of BC and BrC, respectively, assuming WtC does not absorb light. [TC], [BC], [BrC], and [WtC] represent the mass concentration of TC, BC, BrC, and WtC, respectively.

The derived [BC] shows good agreement with [EC], as show in Fig. S2. Similar analysis for the IMPROVE network was reported by June et al. (2020). To compare with the PILS-LWCC-TOC instrument, we calculated the total aerosol absorption at 365 nm by extrapolating the absorption measurements at seven wavelengths with estimated absorption Angstrom exponent (AAE). The total and BC absorption at 365 nm is derived from measured total and BC absorption at 980 nm using total AAE and BC AAE of 0.99 (Chen et al., 2021). Finally, we calculated the absorption coefficient for organic aerosol (OA) at 365 nm by subtracting BC absorption at 365 nm from the Total absorption at the same wavelength. Similar process was done for the calculation of OA absorption due to BrC at other wavelengths. The absorption by dust is considered to be negligible (Fig. S3). The abbreviation of all the given variables is listed in Table S2.

2.3. Plume back trajectory analysis

To estimate the plume origins and transport time, we computed backward plume trajectories based on air mass trajectories using the Hybrid Single Particle Lagrangian Integrated Trajectory (HYSPLIT; Stein et al., 2015) model. The HYSPLIT model is run with two high-resolution meteorological datasets: the High-Resolution Rapid Refresh (HRRR, 3 km) model, and Global Forecast System (GFS, 25 km resolution). An

ensemble of 27 trajectories is initialized at an altitude of ½ mixed layer height over the measurement location in Fairbanks each hour and run backwards for 24 h. For each plume, the source fire is identified from the fire hotspots located along the upwind trajectories (Figs. S4 and S5). When the sky was sufficiently clear, visible imagery from GOES-17 ABI (Geostationary Operational Environmental Satellite, Advanced Baseline Imager), MODIS (Moderate Resolution Imaging Spectroradiometer), and VIIRS (Visible Infrared Imaging Radiometer Suite) satellites are used to corroborate the back trajectory simulations and source fire identification. The age is calculated from the transport time along the central trajectory, averaged between the two meteorological datasets. Uncertainty in the age is determined from the spread in age among trajectory ensemble members. In the trajectory (dark black line), each pink dot (Fig. S4) corresponds to a 1-h interval. We estimated the transport time by tallying the number of pink dots between the fire hotspot and sampling locations.

We used a linear regression model for the estimation of exponential decay (photobleaching) of MAC_{WSOC} during the wildfire events via:

$$ln(y) = a + b(x) \tag{6}$$

$$y = a * e^{bx} (7)$$

where y, and x are response variable (absorption) and predictor variables (transport time from fire plume to sampling location). In equation (6 and 7), a represents the intercept and b represents the coefficient associated with the variable "x" which determine the rate of decay of water soluble BrC per hour.

3. Results and discussion

3.1. Comparison between PILS-LWCC-TOC and filter measurements

We first compare PILS-LWCC-TOC measurements to the filter measurements at NCORE site. Fig. 1a shows the comparison of abswsoc.365 and abs_{OA,365} from PILS-LWCC-TOC and NCORE filters, respectively. Both measurements show similar trends of BrC absorption coefficient at 365 nm (and 405 nm, Fig. S6a), but differ by a factor of 3-4 in magnitude. This could be in part due to that PILS-LWCC-TOC measures only the water-soluble fraction of BrC, while the NCORE filters capture both water soluble and insoluble BrC. We showed in Fig. S7 that water insoluble OC can account for more than 50% of aerosol OC, consistent with previous findings (Yuan et al., 2020; Zeng et al., 2022). We do not find a low bias in the sampling efficiency of PILS system, as WSOC measured by PILS is roughly half of the OC measured from NCORE filters on wildfire days, and water insoluble OC likely makes up to another half of OC during these days (Balachandran et al., 2013). The large discrepancy between two measurements on BrC absorption is consistent with a recent study by Chakrabarty et al. (2023), who identified a type of dark brown carbon that is water insoluble and accounts for up to three quarters of short-wavelength light absorption.

Another difference between these two measurements results from the wavelength dependence of BrC absorption from two measurements. In Fig. 1b, absorption coefficient spectra (and Fig. S6(b) for MAC spectra) from PILS-LWCC-TOC showed a strong wavelength-dependence absorption in the range of 300–400 nm, compared to the filter data derived from extrapolation of measurements at seven wavelengths between 405 and 980 nm. We found a similar wavelength dependence for filter measurements using wavelength pairs of 405 nm and 550 nm. This highlights a potential underestimate of BrC UV absorption using filter measurements and AAE described at visible wavelengths, similar to previous findings (Zeng et al., 2022).

Despite the potential underestimate of abs_{OA} in 300–400 nm range, we observed that OA still accounts for a major fraction of absorption in this wavelength range. Fig. 1c shows the absorption coefficient of OA and BC at 365 nm for the 2019 summer (June and July) based on filter

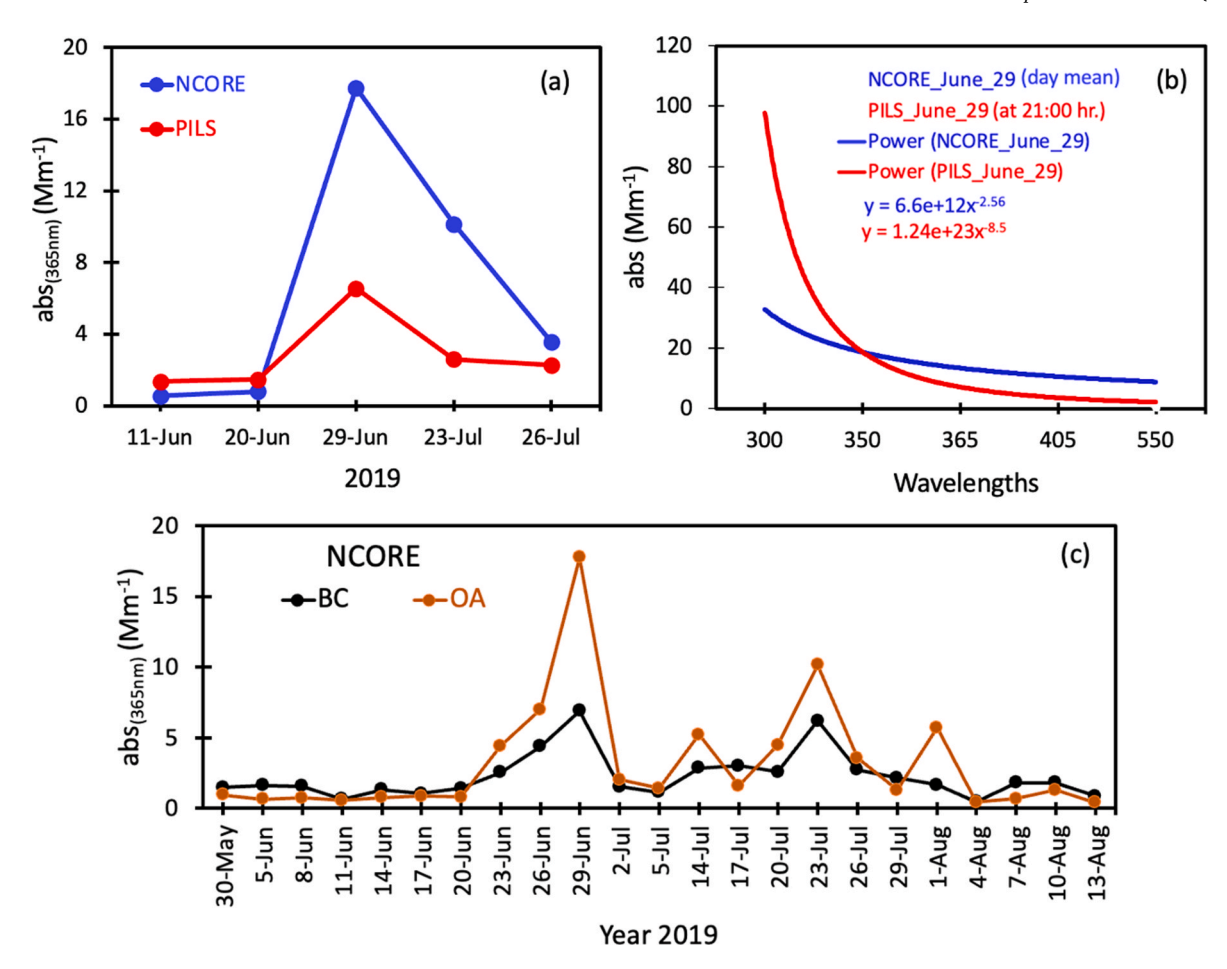


Fig. 1. Comparison of NCORE and PILS-LWCC-TOC measurements. (a) Shows the (with available days) comparison of abs_{WSOC,365} (PILS, red) and abs_{OA,365} (NCORE, blue). (b) Shows the absorption spectra of abs_{WSOC,365} and abs_{OA,365} with wavelength on June 29. The calculation regarding extrapolation of abs from 405 nm to 300 nm is mentioned in Section 2.2. (c) Shows the abs_{OA,365} (brown) and BC absorption (365 nm, black) during June–July 2019 from NCORE.

measurements only. A clear dominance of abs $_{OA}$ with the peak of $\sim 18~Mm^{-1}$ was observed, nearly 3 times the BC absorption coefficient ($\sim 6~Mm^{-1}$). This is mainly due to the fact that the mass of OA was ~ 3 times higher than the mass of BC, consistent with previous boreal smoke studies (June et al., 2020).

3.2. Water soluble brown carbon in summer of 2019

We now further examine PILS-LWCC-TOC data in detail. We have sampled 21 days during the period of June 9 to July 30, 2019 (summarized in Fig. S8 and Table S3). All the available fire hotspots within the wildfire days are highlighted in Fig. S9 and Table S4. Here we compare measurements in two periods to contrast the difference in BrC light absorption and ancillary measurements between with and without wildfire impacts.

Fig. 2 shows the hourly averaged WSOC and, absorption coefficient at 365 nm (abs $_{\rm WSOC,365}$) measured by PILS-LWCC-TOC, along with hourly measurements of NO $_{\rm y}$, CO and PM $_{\rm 2.5}$ from the NCORE site. Case I and Case II correspond to the presence of wildfire and absence of wildfire, respectively. Upwind trajectories for this period are shown in Fig. S5. The wildfire impact was first observed at 17:00 on June 28 and then again around 4:00am on June 29, with increasing PM $_{\rm 2.5}$, CO, and NO $_{\rm y}$ concentrations. The plume intensity reached a maximum on the night of June 29, with PM $_{\rm 2.5}$ over 100 µg m $^{-3}$ and CO close to 1000 ppbv. Fairbanks area was then buried in the plume for a period of almost 24 h. During this period, we see a significant variability on CO, PM $_{\rm 2.5}$ and abs $_{\rm WSOC,365}$. There was a slight decrease in the plume impact during early morning of June 30, but a subsequent resurgence was observed

with some high values recorded between 10:00am to 20:00pm on June 30 with $PM_{2.5}$ –100–150 (μgm^{-3}), CO>1500 (ppbv), WSOC ~ 30 (μgm^{-3}), and $abs_{WSOC,365}$ –25 (Mm^{-1}). We find that WSOC accounts for 20–30% of $PM_{2.5}$ mass concentrations. We also find a positive correlation between $abs_{WSOC,365}$ and CO (Fig. S10), with slopes is comparable to previous studies (Sullivan et al., 2022; Zeng et al., 2022).

In the Case II period (July 25 and 26) period with the absence of wildfire, where a low concentration of CO ($\sim\!100$ ppbv) and $PM_{2.5}$ ($<\!25$ $\mu g~m^{-3}$) were observed, along with low values of WSOC ($<\!10~\mu g~m^{-3}$) and abs_WSOC,365 ($<\!10~Mm^{-1}$). The low abs_WSOC,365 values in the absence of wildfire indicated low background level of BrC in Arctic summer and wildfire smoke is indeed the main source of BrC. A spike during this period with high CO without enhancement of abs_WSOC,365 was likely due to local anthropogenic sources (Fig. 2 and Fig. S11). We find that domestic wood burning has a negligible contribution to $PM_{2.5}$ as $PM_{2.5}$ levels remain markedly low ($<\!10~\mu g~m^{-3}$) throughout the day on clean days (Fig. S8a).

One remarkable feature in Case (I) is the relative stable value of MACWSOC,365 (mass absorption coefficient, MAC) during the plume period from June 29 to June 30. Fig. 2 show that MACWSOC,365 increased from 0.5 m² g⁻¹ to 1 m² g⁻¹ and remained near ~ 1 m² g⁻¹ for over 24 h on 30 June, despite the large variability in PM2.5 and CO concentrations. The fire plume sampled on June 29 likely originated from the Lloyd Mountain fire and it took about 6–7 h for the plume to arrive at the NCORE site. The plume sampled on June 30 likely originated from the Shovel Creek fire (Figs. S4 and S5), mainly from the west side of Fairbanks, and it took about 1–2 h for the plume to arrive at the NCORE site. We find MACWSOC,365 values relatively stable (throughout the plume)

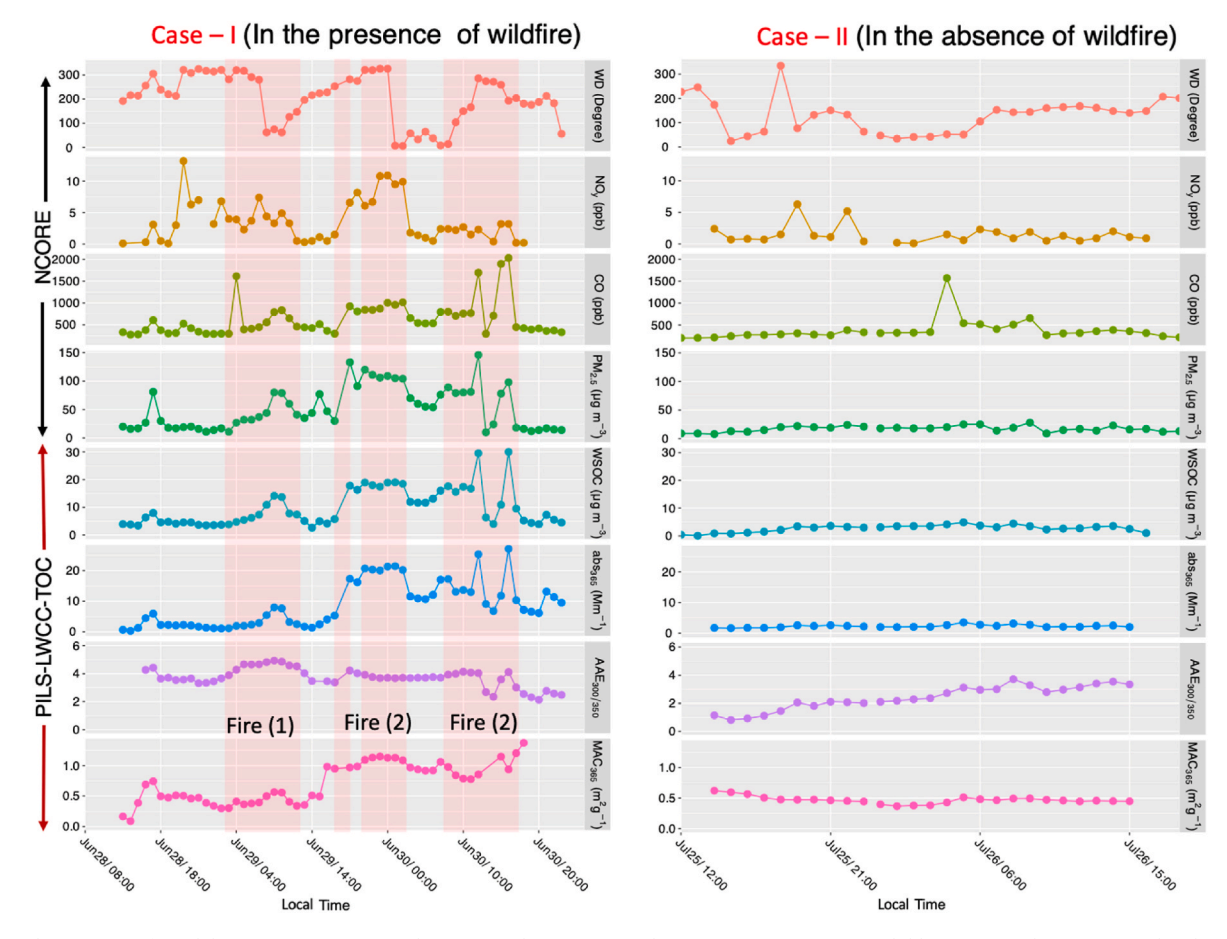


Fig. 2. Hourly variation of wind direction (WD), NOy, carbon monoxide (CO), particulate matter (PM_{2.5}), water soluble organic carbon (WSOC), absorbing angstrom exponent (AAE), absorption coefficient (abs_{WSOC,365}) and mass absorption coefficient (MAC_{WSOC,365}). Shaded box showing the wildfire plumes. Fire (1) corresponds to the Lloyd Mountain fire and Fire (2) corresponds to the Shovel Creek fire.

around $\sim 1~\text{m}^2~\text{g}^{-1}$ even at 4-min resolution (Fig. S12). The difference in calculated MAC_{WSOC,365} between June 29 and 30 could be due to the photobleaching effect, as we showed in Section 3.3 below.

Our calculated MAC_{WSOC,365} of \sim 0.5–1 m² g⁻¹ agrees with previous biomass burning studies in China and the United States (Du et al., 2014; Tang et al., 2020; Xie et al., 2017; Zhang et al., 2011). Similar range of MAC_{WSOC,365} or MAC_{OA,365} (\sim 0.4–1 m² g⁻¹) from biomass burning was also observed in the Arctic (Barrett and Sheesley, 2017; McNaughton et al., 2011; Yue et al., 2019, 2022). The good agreement on MAC_{WSOC,365} between these measurements and measurements in mid-latitude, suggested little difference in MAC_{WSOC,365} in near-UV range between boreal and mid-latitude wildfires (Supplementary Table S5).

We also computed AAE using wavelength pairs of 300 nm and 350 nm. The resulting AAE ranges from 2 to 6 during wildfire events, consistent with previous studies in mid-latitude biomass burning (Table S6). We found that the calculated AAE_{300/350} is relatively stable (~4) during the intense fire events (June 30). However, the AAE can increase by 2–3 units if we choose the wavelength pairs of 300 and 550 nm (Fig. S13), suggesting that the calculated AAE can vary from the choice of wavelength pairs. Therefore, it is possible that the large variability of AAE in Table S6 in part result from the choice of wavelength pairs. We also observed some high AAEs during the period without wildfires (June 25 and 26), suggesting that AAE alone might not be adequate to distinguish the wildfire events.

3.3. Photobleaching effect of BrC (WSOC)

Fig. 3 shows the hourly measured MAC_{WSOC, λ} and Δ abs $_{\lambda}/\Delta$ CO from all the wildfire events, as a function of transport time during the summer

of 2019. To avoid the uncertainty in $MAC_{WSOC,\lambda}$ at low WSOC values, we limited Fig. 3 to data points with $PM_{2.5}$ concentrations exceeding 25 μg m⁻³. For the calculation of $\Delta abs/\Delta CO$, we first compute the background values from the clean periods with CO between 100 and 200 ppbv, leading to background values of CO (162 ppbv) and absorption coefficient (abs = 0.9 Mm⁻¹). The values for ΔCO and Δabs were then determined by subtracting the background values from the ambient values collected during wildfire events. As most wildfires in Alaska take place in interior Alaska (between Alaska range and Brooks Range), we find from HYSPLIT analysis that all the plumes sampled at the Fairbanks NCORE site in this study originated from locations within a few hundred kilometers and were transported to the site within 24 h.

We noticed in Fig. 3a that MAC_{WSOC,365} ranges from \sim 0.2 to 1.2 m² g⁻ ¹ during most fire events, with higher values corresponding to shorter transport times. The events with high MACWSOC.365 values were related the Shovel Creek fire, with a short transport time to the site (1–3 h). The overall time dependence of MAC_{WSOC,365} could be expressed as y = 1.14exp (-0.086 t), suggesting a photochemical lifetime of \sim 12 h for MAC_{WSOC,365} with initial value of $\sim 1.14 \text{ m}^2 \text{ g}^{-1}$. This MAC_{WSOC,365} value is consistent with literature values (Tang et al., 2020; Washenfelder et al., 2022; Xie et al., 2017). The decreased of $MAC_{WSOC,365}$ values with longer transport time are consistent with the photochemical bleaching from some field measurements (Forrister et al., 2015). In Fig. 3a, much lower MACWSOC.365 were also found for the fires on July 23 and 24, although the ages for these events are highly uncertain due to multiple wildfires plumes potentially contributing to the smoke (Fig. S14). In contrast to recent studies in mid-latitudes (Sullivan et al., 2022; Washenfelder et al., 2022; Zeng et al., 2022), our overall results suggest a photochemical bleaching in the first few hours and slowing after the 10

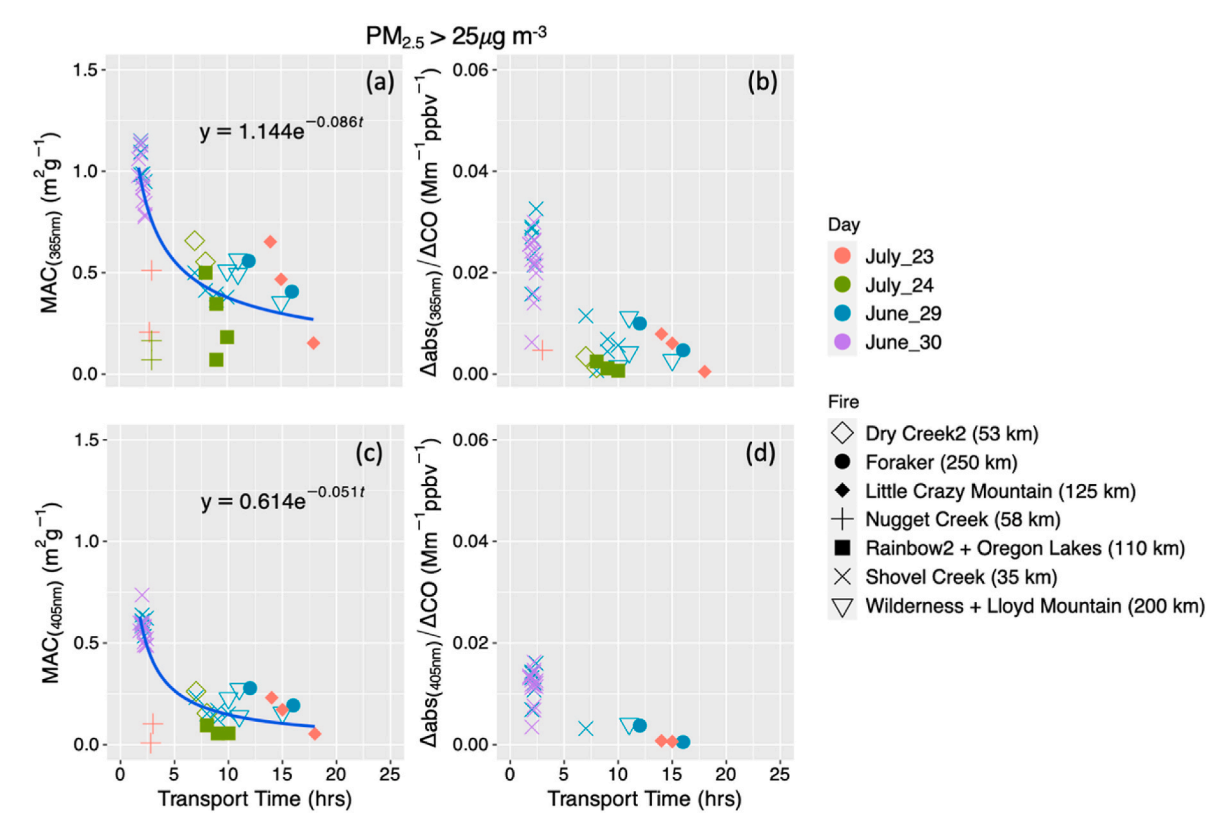


Fig. 3. Measured MAC_{WSOC} and Δ abs_{wsoc}/ Δ CO from two wavelengths, 365 nm (a, b) and 405 nm (c, d). Marker shapes signify the source fire names with distance (km) from the sampling location (Fairbanks). Marker colors indicate the different events.

h. A certain fraction of BrC appears to remain stable without further photobleaching. This remainder of BrC absorptivity can be due to the presence of stable, high molecular weight chromophores and aromatic compounds (Forrister et al., 2015; Liu et al., 2016; Wong et al., 2019; Di Lorenzo et al., 2017).

We found a similar behavior in $\triangle abs_{WSOC,365}/\triangle CO$. Fig. 3b shows that $\Delta abs_{WSOC,365}/\Delta CO$ ranges was from ~ 0.02 to $0.04~\mathrm{Mm}^{-1}~\mathrm{ppbv}^{-1}$, during the initial 1-5 h of transport time for relatively fresh smoke. Compared to the PILS based studies in mid-latitudes, our Δabs_{WSOC.365}/ Δ CO values (~0–0.04 Mm⁻¹ ppbv⁻¹) appears to be in the lower end of those reported from FIREX-AQ ($\sim 0-0.1 \text{ Mm}^{-1} \text{ ppbv}^{-1}$) (Sullivan et al., 2022; Zeng et al., 2022) and WE-CAN ($\sim 0-0.3 \text{ Mm}^{-1} \text{ ppbv}^{-1}$) (Washenfelder et al., 2022). The differences in $\Delta abs_{WSOC, 365}/\Delta CO$ values could also be related to the different background values used for calculating $\Delta abs_{WSOC,365}$ and ΔCO . Another major difference lies in the timing of photobleaching as WE-CAN and FIREX-AQ reported no significant photobleaching in the first 5-10 h, followed by photobleaching after that. The different behaviors between mid and high latitude fires are unclear but could be due to differences in chemical composition or atmospheric conditions (Lee et al., 2014; Forrister et al., 2015; Zhao et al., 2015; Liu et al., 2016; Wong et al., 2017; Di Lorenzo et al., 2017), as well as difference in sampling methods. Note that our data is based on the sampling from multiple plumes at a fixed site downwind of plumes, while Zeng et al. (2022) and Washenfelder et al. (2022) were based on single plume. In addition, BrC photobleaching can be enhanced by the prolonged sunlight exposure at high latitudes in summer, as well as less flux attenuation inside plumes due to smoldering conditions (Genet et al., 2018; Schmale et al., 2018; Zheng et al., 2018).

Compared to MAC_{WSOC,365}, we find that the absorption at 405 nm decays at a slower rate. We show in Fig. 3c and d that MAC_{WSOC,405} measured by PILS-LWCC-TOC could be described as a function of transport time, $y = 0.614 \exp{(-0.051x)}$. This indicates the absorption of BrC at 405 nm undergoes a slower rate of photobleaching, with a

lifetime of \sim 20 h and initial value of \sim 0.6 m² g⁻¹. The longer lifetime of MAC_{WSOC,405} compared to MAC_{WSOC,365} is in contrast to FIREX-AQ study by Sullivan et al. (2022) that reported no photobleaching up to 9 h at both 365 and 405 nm from PILS. This difference between high latitude and mid-latitude could be possibly related to low MCE (modified combustion efficiency) due to smoldering combustion (Zheng et al., 2018).

4. Conclusion

Arctic region is experiencing warming at a rate that is four times faster than the rest of the world (Chylek et al., 2022; Rantanen et al., 2022). One consequence is the increasing wildfire activities in Arctic region. To what extent the wildfire emissions affect radiative budget in Arctic region remains largely uncertain. In the summer of 2019, we deployed a set of instruments, PILS-LWCC-TOC in downtown Fairbanks, combined with multi-wavelength absorption measurements of filters between 2016 and 2019, to examine the optical properties of BrC during wildfire events in Alaska summer.

We show that the $MAC_{WSOC,365}$ ranges from 0.5 to 1 m² g⁻¹, with $MAC_{WSOC,365}$ close to 1 m² g⁻¹ for fresh smoke in boreal fires (Fig. 3). Remarkably our measured $MAC_{WSOC,365}$ for fresh plumes are in good agreement with previous studies (Table S5). The wide range of measured $MAC_{WSOC,365}$ values in our study results from different photochemical ages of wildfire plume sampled at the Fairbanks site. With all sampled plumes combined, we observed a rapid photobleaching mainly within initial 5 h for water soluble BrC, with a photochemical lifetime of ~12 h at 365 nm and ~20 h at 405 nm. The photobleaching appear to be at odds with recent field studies on biomass burning plumes in midlatitudes (Washenfelder et al., 2022; Zeng et al., 2022).

We further compared PILS-LWCC-TOC measurements with absorption measurements on filters collected at the same location. We found that water soluble organic aerosol light absorption comprised 20–25% of total organic aerosol absorption indicating the importance of water

insoluble brown carbon. This reveals a significant insoluble organic aerosol fraction not measurable by PILS-LWCC-TOC instrument that can account for the majority of organic aerosol absorption in the near UV–visible range (Chakrabarty et al., 2023). In addition, PILS-LWCC-TOC instrument show much stronger wavelength dependence in the 300–400 nm range than the derived wavelength-dependence from filter measurements, suggesting a much stronger absorption of BrC in the near UV–visible range than current estimates from measurements at visible wavelengths (Zeng et al., 2022). Overall, we show from filter data that the absorption by organic aerosols still dominates over BC in the near UV–visible range.

To our knowledge, this work represents the first in situ measurements of water-soluble brown carbon for the boreal forest fires in North America. While the BrC optical properties in North America boreal fires show some similarities to the ones from mid-latitude wildfire, we show that BrC accounts for the majority of carbonaceous aerosols in the near UV–visible range. In fact, BrC can further contribute to the snow melting once they are deposited to snow surface (Brown et al., 2022). Our work highlights the importance to include the BrC in current climate models to better represent the radiative budget in the Arctic region.

CRediT authorship contribution statement

Kunal Bali: Conceptualization, Data curation, Formal analysis, Methodology, Visualization, Writing – original draft, Investigation. Sujai Banerji: Formal analysis, Methodology. James R. Campbell: Data curation, Methodology. Aachal Vallabhbhai Bhakta: Methodology, Visualization. L.-W. Antony Chen: Formal analysis, Methodology, Writing – review & editing. Christopher D. Holmes: Methodology, Visualization, Writing – review & editing. Jingqiu Mao: Conceptualization, Data curation, Formal analysis, Funding acquisition, Investigation, Methodology, Project administration, Supervision, Writing – review & editing.

Declaration of competing interest

The authors confirm that they do not have any known financial or personal conflicts of interest that could be perceived as having an impact on the integrity of the work presented in this paper.

Data availability

Data will be made available on request.

Acknowledgement

KB and JM are supported by NSF grant AGS-2026821. CDH was supported by NASA grant 80 NSSC18K0625. We acknowledge Rodney Weber at Georgia Tech for help with the PILS-LWCC-TOC field deployment.

Appendix A. Supplementary data

Supplementary data to this article can be found online at https://doi.org/10.1016/j.atmosenv.2024.120436.

References

- Akagi, S.K., Yokelson, R.J., Wiedinmyer, C., Alvarado, M.J., Reid, J.S., Karl, T., Crounse, J.D., Wennberg, P.O., 2011. Emission factors for open and domestic biomass burning for use in atmospheric models. Atmos. Chem. Phys. 11, 4039–4072. https://doi.org/10.5194/acp-11-4039-2011.
- Alaska Division of Forestry: 2019. available at: https://forestry.alaska.gov/Assets/pdfs/overview/2019%20FOR%20Annual%20Report%20WEB.pdf.
- Andreae, M.O., Gelencser, A., 2006. Black carbon or brown carbon? The nature of light-absorbing carbonaceous aerosols. Atmos. Chem. Phys. 6, 3131–3148. https://doi.org/10.5194/acp-6-3131-2006.

- Barrett, T.E., Sheesley, R.J., 2017. Year-round optical properties and source characterization of Arctic organic carbon aerosols on the North Slope Alaska.
 J. Geophys. Res. Atmos. 122, 9319–9331. https://doi.org/10.1002/2016JD026194.
 Balachandran, S., Pachon, J.E., Lee, S., Oakes, M.M., Rastogi, N., Shi, W., Tagaris, E.,
- Balachandran, S., Pachon, J.E., Lee, S., Oakes, M.M., Rastogi, N., Shi, W., Tagaris, E., Yan, B., Davis, A., Zhang, X., Weber, R.J., 2013. Particulate and gas sampling of prescribed fires in South Georgia, USA. Atmos. Environ. 81, 125–135.
- Bond, T.C., Anderson, T.L., Campbell, D., 1999. Calibration and intercomparison of filter-based measurements of visible light absorption by aerosols. Aerosol. Sci. Technol. 30, 582–600. https://doi.org/10.1080/027868299304435.
- Brown, H., Wang, H., Flanner, M., Liu, X., Singh, B., Zhang, R., Yang, Y., Wu, M., 2022. Brown carbon fuel and emission source attributions to global snow darkening effect. J. Adv. Model. Earth Syst. 14, e2021MS002768 https://doi.org/10.1029/ 2021MS002768
- Chakrabarty, R.K., Gyawali, M., Yatavelli, R.L.N., Pandey, A., Watts, A.C., Knue, J., Chen, L.-W.A., Pattison, R.R., Tsibart, A., Samburova, V., Moosmüller, H., 2016. Brown carbon aerosols from burning of boreal peatlands: microphysical properties, emission factors, and implications for direct radiative forcing. Atmos. Chem. Phys. 16, 3033–3040. https://doi.org/10.5194/acp-16-3033-2016.
- Chakrabarty, R.K., Shetty, N.J., Thind, A.S., Beeler, P., Sumlin, B.J., Zhang, C., Liu, P., Idrobo, J.C., Adachi, K., Wagner, N.L., Schwarz, J.P., Ahern, A., Sedlacek, A.J., Lambe, A., Daube, C., Lyu, M., Liu, C., Herndon, S., Onasch, T.B., Mishra, R., 2023. Shortwave absorption by wildfire smoke dominated by dark brown carbon. Nat. Geosci. 16, 683–688. https://doi.org/10.1038/s41561-023-01237-9.
- Chen, L.-W.A., Chow, J.C., Wang, X., Cao, J., Mao, J., Watson, J.G., 2021. Brownness of organic aerosol over the United States: evidence for seasonal biomass burning and photobleaching effects. Environ. Sci. Technol. 55, 8561–8572. https://doi.org/ 10.1021/acs.est.0c08706.
- Chen, Y., Bond, T.C., 2010. Light absorption by organic carbon from wood combustion. Atmos. Chem. Phys. 10, 1773–1787. https://doi.org/10.5194/acp-10-1773-2010.
- Chen, L.W.A., Chow, J.C., Wang, X.L., Robles, J.A., Sumlin, B.J., Lowenthal, D.H., Zimmermann, R., Watson, J.G., 2015. Multi-wavelength optical measurement to enhance thermal/optical analysis for carbonaceous aerosol. Atmos. Meas. Tech. 8, 451–461. https://doi.org/10.5194/amt-8-451-2015.
- Chow, J.C., Wang, X., Sumlin, B.J., Gronstal, S.B., Chen, L.-W.A., Trimble, D.L., Kohl, S. D., Mayorga, S.R., Riggio, G., Hurbain, P.R., Johnson, M., Zimmermann, R., Watson, J.G., 2015. Optical calibration and equivalence of a multiwavelength thermal/optical carbon analyzer. Aerosol Air Qual. Res. 15, 1145–1159. https://doi.org/10.4209/aagr.2015.02.0106.
- Chylek, P., Folland, C., Klett, J.D., Wang, M., Hengartner, N., Lesins, G., Dubey, M.K., 2022. Annual mean arctic amplification 1970–2020: observed and simulated by CMIP6 climate models. Geophys. Res. Lett. 49, e2022GL099371 https://doi.org/ 10.1029/2022GL099371.
- Corr, C.A., Hall, S.R., Ullmann, K., Anderson, B.E., Beyersdorf, A.J., Thornhill, K.L., Cubison, M.J., Jimenez, J.L., Wisthaler, A., Dibb, J.E., 2012. Spectral absorption of biomass burning aerosol determined from retrieved single scattering albedo during ARCTAS. Atmos. Chem. Phys. 12, 10505–10518. https://doi.org/10.5194/acp-12-10505-2012.
- Deshmukh, D.K., Haque, M.M., Kim, Y., Kawamura, K., 2019. Organic tracers of fine aerosol particles in central Alaska: summertime composition and sources. Atmos. Chem. Phys. 19, 14009–14029. https://doi.org/10.5194/acp-19-14009-2019.
- Di Lorenzo, R.A., Washenfelder, R.A., Attwood, A.R., Guo, H., Xu, L., Ng, N.L., Weber, R. J., Baumann, K., Edgerton, E., Young, C.J., 2017. Molecular-size-separated brown carbon absorption for biomass-burning aerosol at multiple field sites. Environ. Sci. Technol. 51, 3128–3137. https://doi.org/10.1021/acs.est.6b06160.
- Du, Z., He, K., Cheng, Y., Duan, F., Ma, Y., Liu, J., Zhang, X., Zheng, M., Weber, R., 2014. A yearlong study of water-soluble organic carbon in Beijing II: Light absorption properties, 89, 235–241. https://doi.org/10.1016/j.atmosenv.2014.02.022. Elsevier Enhanced Reader.
- Feng, Y., Ramanathan, V., Kotamarthi, V.R., 2013. Brown carbon: a significant atmospheric absorber of solar radiation? Atmos. Chem. Phys. 13, 8607–8621. https://doi.org/10.5194/acp-13-8607-2013.
- Fleming, L.T., Lin, P., Roberts, J.M., Selimovic, V., Yokelson, R., Laskin, J., Laskin, A., Nizkorodov, S.A., 2020. Molecular composition and photochemical lifetimes of brown carbon chromophores in biomass burning organic aerosol. Atmos. Chem. Phys. 20, 1105–1129. https://doi.org/10.5194/acp-20-1105-2020.
- Forrister, H., Liu, J., Scheuer, E., Dibb, J., Ziemba, L., Thornhill, K.L., Anderson, B., Diskin, G., Perring, A.E., Schwarz, J.P., Campuzano-Jost, P., Day, D.A., Palm, B.B., Jimenez, J.L., Nenes, A., Weber, R.J., 2015. Evolution of brown carbon in wildfire plumes. Geophys. Res. Lett. 42, 4623–4630. https://doi.org/10.1002/2015.0629073.
- Genet, H., He, Y., Lyu, Z., McGuire, A.D., Zhuang, Q., Clein, J., D'Amore, D., Bennett, A., Breen, A., Biles, F., Euskirchen, E.S., Johnson, K., Kurkowski, T., (Kushch) Schroder, S., Pastick, N., Rupp, T.S., Wylie, B., Zhang, Y., Zhou, X., Zhu, Z., 2018. The role of driving factors in historical and projected carbon dynamics of upland ecosystems in Alaska. Ecol. Applications 28, 5–27. https://doi.org/10.1002/eap.1641.
- Hansen, A.D.A., Rosen, H., Novakov, T., 1984. The aethalometer an instrument for the real-time measurement of optical absorption by aerosol particles. Sci. Total Environ. 36, 191–196. https://doi.org/10.1016/0048-9697(84)90265-1.
- Healy, R.M., Wang, J.M., Jeong, C.-H., Lee, A.K.Y., Willis, M.D., Jaroudi, E., Zimmerman, N., Hilker, N., Murphy, M., Eckhardt, S., Stohl, A., Abbatt, J.P.D., Wenger, J.C., Evans, G.J., 2015. Light-absorbing properties of ambient black carbon and brown carbon from fossil fuel and biomass burning sources: light-absorbing properties OF BC. J. Geophys. Res. Atmos. 120, 6619–6633. https://doi.org/ 10.1002/2015JD023382.

- Hecobian, A., Zhang, X., Zheng, M., Frank, N., Edgerton, E.S., Weber, R.J., 2010. Water-Soluble Organic Aerosol material and the light-absorption characteristics of aqueous extracts measured over the Southeastern United States. Atmos. Chem. Phys. 10, 5965–5977. https://doi.org/10.5194/acp-10-5965-2010.
- June, N.A., Wang, Xuan, Chen, L.-W.A., Chow, J.C., Watson, J.G., Wang, Xiaoliang, Henderson, B.H., Zheng, Y., Mao, J., 2020. Spatial and temporal variability of Brown carbon in the United States: implications for direct radiative effects. Geophys. Res. Lett. 47, e2020GL090332 https://doi.org/10.1029/2020GL090332.
- Kristiansen, N.I., Stohl, A., Olivié, D.J.L., Croft, B., Søvde, O.A., Klein, H., Christoudias, T., Kunkel, D., Leadbetter, S.J., Lee, Y.H., Zhang, K., Tsigaridis, K., Bergman, T., Evangeliou, N., Wang, H., Ma, P.-L., Easter, R.C., Rasch, P.J., Liu, X., Pitari, G., Di Genova, G., Zhao, S.Y., Balkanski, Y., Bauer, S.E., Faluvegi, G.S., Kokkola, H., Martin, R.V., Pierce, J.R., Schulz, M., Shindell, D., Tost, H., Zhang, H., 2016. Evaluation of observed and modelled aerosol lifetimes using radioactive tracers of opportunity and an ensemble of 19 global models. Atmos. Chem. Phys. 16, 3525–3561. https://doi.org/10.5194/acp-16-3525-2016.
- Lack, D.A., Lovejoy, E.R., Baynard, T., Pettersson, A., Ravishankara, A.R., 2006. Aerosol absorption measurement using photoacoustic spectroscopy: sensitivity, calibration. and Uncertainty Developments 40, 697–708. https://doi.org/10.1080/ 0275682060092017
- Laskin, A., Laskin, J., Nizkorodov, S.A., 2015. Chemistry of atmospheric Brown carbon. Chem. Rev. 115, 4335–4382. https://doi.org/10.1021/cr5006167.
- Lee, H.J. (Julie), Aiona, P.K., Laskin, A., Laskin, J., Nizkorodov, S.A., 2014. Effect of solar radiation on the optical properties and molecular composition of laboratory proxies of atmospheric Brown carbon. Environ. Sci. Technol. 48, 10217–10226. https://doi. org/10.1021/es502515r.
- Lin, P., Aiona, P.K., Li, Y., Shiraiwa, M., Laskin, J., Nizkorodov, S.A., Laskin, A., 2016. Molecular characterization of Brown carbon in biomass burning aerosol particles. Environ. Sci. Technol. 50, 11815–11824. https://doi.org/10.1021/acs.est.6b03024.
- Liu, J., Lin, P., Laskin, A., Laskin, J., Kathmann, S.M., Wise, M., Caylor, R., Imholt, F., Selimovic, V., Shilling, J.E., 2016. Optical properties and aging of light-absorbing secondary organic aerosol. Atmos. Chem. Phys. 16, 12815–12827. https://doi.org/ 10.5194/acp-16-12815-2016.
- McCarty, J.L., Aalto, J., Paunu, V.-V., Arnold, S.R., Eckhardt, S., Klimont, Z., Fain, J.J., Evangeliou, N., Venäläinen, A., Tchebakova, N.M., Parfenova, E.I., Kupiainen, K., Soja, A.J., Huang, L., Wilson, S., 2021. Reviews and syntheses: Arctic fire regimes and emissions in the 21st century. Biogeosciences 18, 5053–5083. https://doi.org/10.5194/bg-18-5053-2021.
- McNaughton, C.S., Clarke, A.D., Freitag, S., Kapustin, V.N., Kondo, Y., Moteki, N., Sahu, L., Takegawa, N., Schwarz, J.P., Spackman, J.R., Watts, L., Diskin, G., Podolske, J., Holloway, J.S., Wisthaler, A., Mikoviny, T., de Gouw, J., Warneke, C., Jimenez, J., Cubison, M., Howell, S.G., Middlebrook, A., Bahreini, R., Anderson, B. E., Winstead, E., Thornhill, K.L., Lack, D., Cozic, J., Brock, C.A., 2011. Absorbing aerosol in the troposphere of the Western Arctic during the 2008 ARCTAS/ARCPAC airborne field campaigns. Atmos. Chem. Phys. 11, 7561–7582. https://doi.org/10.5194/acp-11-7561-2011.
- Petzold, A., Schönlinner, M., 2004. Multi-angle absorption photometry—a new method for the measurement of aerosol light absorption and atmospheric black carbon.

 J. Aerosol Sci. 35, 421–441. https://doi.org/10.1016/j.jaerosci.2003.09.005.
- Rantanen, M., Karpechko, A.Yu, Lipponen, A., Nordling, K., 2022. The Arctic Has Warmed Nearly Four Times Faster than the Globe since 1979.
- Saleh, R., Hennigan, C.J., McMeeking, G.R., Chuang, W.K., Robinson, E.S., Coe, H., Donahue, N.M., Robinson, A.L., 2013. Absorptivity of brown carbon in fresh and photo-chemically aged biomass-burning emissions. Atmos. Chem. Phys. 13, 7683–7693. https://doi.org/10.5194/acp-13-7683-2013.
- Saleh, R., Robinson, E.S., Tkacik, D.S., Ahern, A.T., Liu, S., Aiken, A.C., Sullivan, R.C., Presto, A.A., Dubey, M.K., Yokelson, R.J., Donahue, N.M., Robinson, A.L., 2014. Brownness of organics in aerosols from biomass burning linked to their black carbon content. Nat. Geosci. 7, 647–650. https://doi.org/10.1038/ngeo2220.
- Schmale, J., Arnold, S.R., Law, K.S., Thorp, T., Anenberg, S., Simpson, W.R., Mao, J., Pratt, K.A., 2018. Local arctic air pollution: a neglected but serious problem. Earth's Future 6, 1385–1412. https://doi.org/10.1029/2018EF000952.
- Soleimanian, E., Mousavi, A., Taghvaee, S., Shafer, M.M., Sioutas, C., 2020. Impact of secondary and primary particulate matter (PM) sources on the enhanced light absorption by brown carbon (BrC) particles in central Los Angeles | Elsevier Enhanced Reader. Sci. Total Environ. 705, 135902 https://doi.org/10.1016/j. scitotenv.2019.135902.
- Stein, A.F., Draxler, R.R., Rolph, G.D., Stunder, B.J.B., Cohen, M.D., Ngan, F., 2015. NOAA's HYSPLIT atmospheric transport and dispersion modeling system. Bull. Am. Meteorol. Soc. 96, 2059–2077. https://doi.org/10.1175/BAMS-D-14-00110.1.
- Sullivan, A.P., Pokhrel, R.P., Shen, Y., Murphy, S.M., Toohey, D.W., Campos, T., Lindaas, J., Fischer, E.V., Collett Jr., J.L., 2022. Examination of brown carbon absorption from wildfires in the western US during the WE-CAN study. Atmos. Chem. Phys. 22, 13389–13406. https://doi.org/10.5194/acp-22-13389-2022.
- Sullivan, A.P., Weber, R.J., Clements, A.L., Turner, J.R., Bae, M.S., Schauer, J.J., 2004. A method for on-line measurement of water-soluble organic carbon in ambient aerosol particles: results from an urban site. Geophys. Res. Lett. 31 https://doi.org/ 10.1029/2004GL019681.
- Sumlin, B.J., Pandey, A., Walker, M.J., Pattison, R.S., Williams, B.J., Chakrabarty, R.K., 2017. Atmospheric photooxidation diminishes light absorption by primary Brown carbon aerosol from biomass burning. Environ. Sci. Technol. Lett. 4, 540–545. https://doi.org/10.1021/acs.estlett.7b00393.
- Tang, Jiao, Li, J., Su, T., Han, Y., Mo, Y., Jiang, H., Cui, M., Jiang, B., Chen, Y., Tang, Jianhui, Song, J., Peng, P., Zhang, G., 2020. Molecular compositions and optical properties of dissolved brown carbon in biomass burning, coal combustion, and vehicle emission aerosols illuminated by excitation–emission matrix

- spectroscopy and Fourier transform ion cyclotron resonance mass spectrometry analysis. Atmos. Chem. Phys. 20, 2513–2532. https://doi.org/10.5194/acp-20-2513-2009.
- Turetsky, M., Benscoter, B., Page, S., 2014. Global vulnerability of peatlands to fire and carbon loss. Nat. Geosci. 8, 11–14. https://doi.org/10.1038/ngeo2325.
- Turetsky, M., Kane, S., Harden, W., 2010. Recent acceleration of biomass burning and carbon losses in Alaskan forests and peatlands, 2011 Nat. Geosci. 4, 27–31. https:// doi.org/10.1038/ngeo1027, 10.1038/ngeo1027. Nature Geoscience 4, 27–31.
- Veraverbeke, S., Rogers, B.M., Goulden, M.L., Jandt, R.R., Miller, C.E., Wiggins, E.B., Randerson, J.T., 2017. Lightning as a major driver of recent large fire years in North American boreal forests. Nat. Clim. Change 7, 529–534. https://doi.org/10.1038/ nclimate3339
- Washenfelder, R.A., Azzarello, L., Ball, K., Brown, S.S., Decker, Z.C.J., Franchin, A., Fredrickson, C.D., Hayden, K., Holmes, C.D., Middlebrook, A.M., Palm, B.B., Pierce, R.B., Price, D.J., Roberts, J.M., Robinson, M.A., Thornton, J.A., Womack, C. C., Young, C.J., 2022. Complexity in the evolution, composition, and spectroscopy of Brown carbon in aircraft measurements of wildfire plumes. Geophys. Res. Lett. 49, e2022GL098951 https://doi.org/10.1029/2022GL098951.
- Washenfelder, R.A., Flores, J.M., Brock, C.A., Brown, S.S., Rudich, Y., 2013. Broadband measurements of aerosol extinction in the ultraviolet spectral region. Atmos. Meas. Tech. 6, 861–877. https://doi.org/10.5194/amt-6-861-2013.
- Watson, J.G., Cao, J., Chen, L.-W.A., Wang, Q., Tian, J., Wang, X., Gronstal, S., Ho, S.S. H., Watts, A.C., Chow, J.C., 2019. Gaseous, PM_{2.5} mass, and speciated emission factors from laboratory chamber peat combustion. Atmos. Chem. Phys. 19, 14173–14193. https://doi.org/10.5194/acp-19-14173-2019.
- Weber, R.J., Orsini, D., Daun, Y., Lee, Y.-N., Klotz, P.J., Brechtel, F., 2001. A particle-into-liquid collector for rapid measurement of aerosol bulk chemical composition. Aerosol. Sci. Technol. 35, 718–727. https://doi.org/10.1080/02786820152546761.
- Wong, J.P.S., Nenes, A., Weber, R.J., 2017. Changes in light absorptivity of molecular weight separated Brown carbon due to photolytic aging. Environ. Sci. Technol. 51, 8414–8421. https://doi.org/10.1021/acs.est.7b01739.
- Wong, J.P.S., Tsagkaraki, M., Tsiodra, I., Mihalopoulos, N., Violaki, K., Kanakidou, M., Sciare, J., Nenes, A., Weber, R.J., 2019. Atmospheric evolution of molecular-weight-separated brown carbon from biomass burning. Atmos. Chem. Phys. 19, 7319–7334. https://doi.org/10.5194/acp-19-7319-2019.
- Xie, M., Hays, M.D., Holder, A.L., 2017. Light-absorbing organic carbon from prescribed and laboratory biomass burning and gasoline vehicle emissions. Sci. Rep. 7, 7318. https://doi.org/10.1038/s41598-017-06981-8.
- Yan, J., Wang, X., Gong, P., Wang, C., Cong, Z., 2018. Review of brown carbon aerosols: recent progress and perspectives. Sci. Total Environ. 634, 1475–1485. https://doi. org/10.1016/j.scitoteny.2018.04.083.
- Yuan, W., Huang, R.-J., Yang, L., Guo, J., Chen, Z., Duan, J., Wang, T., Ni, H., Han, Y., Li, Y., Chen, Q., Chen, Y., Hoffmann, T., O'Dowd, C., 2020. Characterization of the light-absorbing properties, chromophore composition and sources of brown carbon aerosol in Xi'an, northwestern China. Atmos. Chem. Phys. 20, 5129–5144. https://doi.org/10.5194/acp-20-5129-2020.
- Yue, S., Bikkina, S., Gao, M., Barrie, L.A., Kawamura, K., Fu, P., 2019. Sources and radiative absorption of water-soluble Brown carbon in the high arctic atmosphere. Geophys. Res. Lett. 46, 14881–14891. https://doi.org/10.1029/2019GL085318.
- Yue, S., Zhu, J., Chen, S., Xie, Q., 2022. Brown carbon from biomass burning imposes strong circum-Arctic warming. One Earth 5, 293–304. https://doi.org/10.1016/j. oneear.2022.02.006.
- Zeng, L., Dibb, J., Scheuer, E., Katich, J.M., Schwarz, J.P., Bourgeois, I., Peischl, J., Ryerson, T., Warneke, C., Perring, A.E., Diskin, G.S., DiGangi, J.P., Nowak, J.B., Moore, R.H., Wiggins, E.B., Pagonis, D., Guo, H., Campuzano-Jost, P., Jimenez, J.L., Xu, L., Weber, R.J., 2022. Characteristics and evolution of brown carbon in western United States wildfires. Atmos. Chem. Phys. 22, 8009–8036. https://doi.org/ 10.5194/acp-22-8009-2022.
- Zeng, L., Sullivan, A.P., Washenfelder, R.A., Dibb, J., Scheuer, E., Campos, T.L., Katich, J. M., Levin, E., Robinson, M.A., Weber, R.J., 2021. Assessment of online water-soluble brown carbon measuring systems for aircraft sampling. Atmos. Meas. Tech. 14, 6357–6378. https://doi.org/10.5194/amt-14-6357-2021.
- Zhang, X., Lin, Y.-H., Surratt, J.D., Weber, R.J., 2013. Sources, composition and absorption ångström exponent of light-absorbing organic components in aerosol extracts from the Los Angeles basin. Environ. Sci. Technol. 47, 3685–3693. https://doi.org/10.1021/es305047b.
- Zhang, X., Lin, Y.-H., Surratt, J.D., Zotter, P., Prévôt, A.S.H., Weber, R.J., 2011. Light-absorbing soluble organic aerosol in Los Angeles and Atlanta: A contrast in secondary organic aerosol. Geophys. Res. Lett. 38 https://doi.org/10.1029/2011GL049385
- Zeng, L., Zhang, A., Wang, Y., Wagner, N.L., Katich, J.M., Schwarz, J.P., Schill, G.P., Brock, C., Froyd, K.D., Murphy, D.M., Williamson, C.J., Kupc, A., Scheuer, E., Dibb, J., Weber, R.J., 2020. Global measurements of brown carbon and estimated direct radiative effects. Geophys. Res. Lett. 47 https://doi.org/10.1029/2020GL088747 e2020GL088747.
- Zhang, Y., Forrister, H., Liu, J., Dibb, J., Anderson, B., Schwarz, J.P., Perring, A.E., Jimenez, J.L., Campuzano-Jost, P., Wang, Y., Nenes, A., Weber, R.J., 2017. Top-ofatmosphere radiative forcing affected by brown carbon in the upper troposphere. Nat. Geosci. 10, 486–489. https://doi.org/10.1038/ngeo2960.

- Zhao, R., Lee, A.K.Y., Huang, L., Li, X., Yang, F., Abbatt, J.P.D., 2015. Photochemical processing of aqueous atmospheric brown carbon. Atmos. Chem. Phys. 15, 6087–6100. https://doi.org/10.5194/acp-15-6087-2015.
 Zheng, B., Chevallier, F., Ciais, P., Yin, Y., Wang, Y., 2018. On the role of the flaming to smoldering transition in the seasonal cycle of african fire emissions. Geophys. Res.
- Lett. 45 https://doi.org/10.1029/2018GL079092.
- Zhong, M., Jang, M., 2014. Dynamic light absorption of biomass-burning organic carbon photochemically aged under natural sunlight. Atmos. Chem. Phys. 14, 1517–1525. https://doi.org/10.5194/acp-14-1517-2014.